Universitetet i Stavanger

FACULTY OF SCIENCE AND TECHNOLOGY

MASTER'S THESIS

Study program/specialization: Petroleum technology Drilling and well engineering	Spring semester, 2017 Open
Author: Christian Lysen	…… (signature of author)
Supervisor(s): Bernt Sigve Aadnøy	
Title of master's thesis: Potential of evaporation for geothermal energy exploitation	
Credits: 30 ECTS	
Keywords: Geothermal energy Heat pipes Drilling Renewable energy	Number of pages: 51 + Appendix: 5 Stavanger, 13.06/2017

Abstract

This master thesis investigates the potential of using heat pipes as geothermal heating systems for domestic purposes. The total electric energy consumption in Norway used for heating purposes is estimated to be as much as 100 TWh a year. This means that successful implementation of a new energy system would not only save money for the consumer, but also provide relief to the existing power grids.

To examine the possibility of using heat pipes, a case study is performed based on available models and theory adapted for a Norwegian environment. The system is considered as an array of thermal resistances which control how much heat that is possible to extract from the ground. The energy that is extracted represents a cashflow which makes it possible to investigate the profitability of the system designed in the case.

The case study shows that when drilling an 800 meter well, 86 250 kWh of heat is possible to extract when utilizing a heat pipe system with ammonia as working fluid. The system can supply 4 houses with heat equivalent to what average households use in terms of electric heating. The economic analysis of the system shows that the system is profitable with a net present value of 331 077 NOK. The minimum depth for this system to show profitability is found to be at approximately 300 meters depth.

Though the base case shows profitability, projects like this are highly sensitive to costs related to drilling and selection of materials. The models that are applied do not take into consideration important issues regarding heat pipe operations which add uncertainty to the production numbers. The projects are therefore likely to be economically marginal without any governmental support. The findings in this thesis are still interesting enough to investigate further and develop better models to better understand the working potential of heat pipes as geothermal energy extractors.

Acknowledgments

I would like to use this opportunity to express my sincere gratitude towards my faculty supervisor, Bernt Sigve Aadnøy, for guidance and help during my work with this thesis. He has provided me with useful information and good stories at his office.

This journey started in 2014 when I moved to Stavanger, and without the motivation from my dear family in Bergen, the finish line would have seemed so much further away. A special thank goes to my girlfriend, Julie. Thank you for waiting 3 years so I could study the things that interest me the most.

Table of content

List of figures, plots and tables

Nomenclature

A	Cross sectional area [m^2]
C_p	Specific heat capacity [J kg^{-1} K^{-1}]
D and d	Diameter [m]
H and U	Heat transfer coefficient [W m^{-2} K^{-1}]
h'	Specific enthalpy [J kg^{-1}]
h_{fg}	Latent heat of vaporization [J kg^{-1}]
k	Thermal conductivity [W m^{-1} K^{-1}]
L	Heat pipe length [m]
m	Mass flow rate [kg s^{-1}]
P	Pressure [Pa]
Q	Heat transfer rate [W]
R	Radius [m] or thermal resistance [K W^{-1}]
S	Surface area [m^2]
s	Specific entropy [J kg^{-1} K^{-1}]
T	Temperature [K]
t	Time [s]
W	Work done by the system/process [J]
λ	Material thickness of conductor [m]
μ	Viscosity [N s^{-1} kg^{-1}]
ρ	Density [Kg m^{-3}]
ή	Constant
η	Constant
ς	Constant
Denotations:	
e	Evaporator
c	Condenser
o	Outer
i	Inner
∞	Environment
l	Liquid
v	Vapor
w	Wick

1 Introduction

1.1 Geothermal Energy

For thousands of years have man found the use of geothermal energy for various purposes. North American Indians used hot springs to clean their body and mind [1], and today we see a much stronger focus on exploiting geothermal energy and other renewables in general. According to BPs statistical review for 2016 the average capacity for geothermal energy has increased to 13 GW. United States of America accounts for 28 % of the total capacity alone followed by the Philippines with 15 %. NGU estimates the total energy stored in the earth to be 100 million EJ (10^{26} Joule), enough to satisfy the world energy consumption for the next 300 00 years [2].

Energy from the ground can be divided into two different fields; shallow geothermal energy and deep geothermal energy. Shallow geothermal energy relates to uppermost parts of the subsurface, typically down to approximately 400 to 500 meters. The temperature at this depth is affected by solar radiation and other climate effects such as the local temperature. If a well is drilled beyond this, the temperature will follow the geothermal gradient. The increase in temperature is due to magma intrusions and decay of radioactive isotopes in the rock such as isotopes from Thorium, Potassium and Uranium [3]. The world average geothermal gradient ranges from 20 °C/km to 30 °C/km depending on where the well is located, but may deviate in places with high volcanic activity such as Iceland.

Deep geothermal energy is usually exploited by drilling wells into a reservoir rock and extract a well stream consisting of either liquid water or steam. The power plants in operation today uses one of these three processes:

- Dry steam cycle: this is the oldest principle and directly uses steam as working fluid to feed the turbines. Hot reservoir steam is produced through a well and fed onto a turbine-generator system with high pressure. After the steam has released its kinetic energy to the turbines, it runs through a condenser and turns into liquid phase. The water is then pumped down an injector well back to the reservoir [4].

- Flash steam cycle: the well stream is produced to a separator tank where the pressure is dropped. The pressure drop causes some of the water to flash into vapor and this is then used to turn the turbines. The separator water and working fluid from the turbine outlet is then reunited and pumped back to the reservoir. Most geothermal power plants today work under this principle [4].

- Binary cycle: this is the newest development in power production from geothermal energy. The well stream is produced and its energy is released to a heat exchanger with an evaporation tank standing at the surface. The energy transmitted from the well stream is transferred to another fluid with a much lower boiling point making it to vaporize. The vaporized working fluid is then fed to the turbines and undergoes a condensation process before it is returned to the evaporator tank. The well stream is pumped back into the reservoir like the water in the other steam cycles [4].

1.2 Ground source heat pumps

For shallow geothermal energy, most methods relate to heating purposes such as water- and house heating. The most common method utilizes a ground source heat pump (GSHP). This is a system where a well is drilled 150 to 300 meters down into the soil. Once the well is drilled, a dual pipe (u-tube) is inserted in the well and one can circulate a working fluid in and out of the well. The well is then filled with a thermal grout that offers good thermal connection between the rock and the pipes. The working fluid used in Norwegian conditions is typically water with additives such as glycol to prevent freezing in the system during low surface temperatures. The temperature in the well is normally not high enough to deliver heating by itself, so the working fluid is delivered to an air-water heat pump located top side and the temperature is raised to desired level [5]. The use of GSHPs for heating purposes also allows the heat pump to be reversed during summer seasons when the desired temperature is colder, this is called underground thermal energy storage (UTES) [6].

1.3 Geothermal status and potential in Norway

In 2003, the total energy consumption in Norway was 220 TWh and of this the consumption of electricity accounted for almost 50 %. Of the electricity consumption, 85-90 % was used to heat buildings. Norway has seen a growth in installed heat pumps, and in 2003, a total of 55 100 heat pumps where installed in buildings and houses across the country. The heat pumps where mainly air-source heat pumps and only 5 % where GSHPs [6].

The Norwegian geology consists of bedrock from the Caledonian mountain range with characteristics such as low permeability and porosity. Despite that Norway is an oil producing nation, there are no sedimentary basins onshore. This makes drilling a costly operation, and though there has been an increase in GSHP installations, the potential for geothermal energy is to be considered low temperature only (<100 °C). As of 2010, the average geothermal energy production was 2300 GWh/year and the installed capacity is estimated to be 1300 MW (thermal) from mostly GSHPs [7].

2 Heat pipe systems

This section will cover an overview of different heat pipe systems, applications and system limitations.

2.1 The heat pipe principle

Heat pipes are passive devices that does not need a pump to circulate the working fluid, the evaporation and condensation of the working fluid will ensure this to happen [8]. To understand the working principle of a heat pipe, one can consider a pipe or a cylinder with both of its ends closed. The cylinder is then charged with a working fluid that will act as the thermal energy carrier under the right conditions (pressure and temperature). If the cylinder is exposed to an area where a temperature difference is present over the pipe, a movement of energy will start to happen.

The way this works is that the hot end of cylinder will evaporate the working fluid inside, and the rise in pressure will make the newly formed vapor travel across the cylinder towards the cooler section of pipe. When the vapor containing energy reaches this side and gets cooled down due to the temperature difference in that end of the pipe, the vapor will release its energy to equalize the temperature difference [9] and condense back to liquid state.

When in liquid state, the working fluid travels back to the evaporator section of the pipe through a wick structure in the pipe wall. Due to capillary forces acting in the pores of this structure, the pipe wall now acts as a pump driven by a pressure difference created by the movement of fluids in the pipe. As the working fluid reaches back to the evaporator section, the whole process starts over again. Because of the utilization of a wick structure, heat pipes can operate normally when oriented horizontally and even if inclined [10].

2.2 Gravity assisted heat pipes

Heat pipes that does not involve the utilization of wick structures are called wick-less heat pipes or thermosyphons [10]. This is a device that operates under much the same conditions as a conventional heat pipe, but lacks the properties of a wick structure in the pipe wall. The driving force in these devices is gravity. This means in general that the condensed liquid in the condenser section can flow back freely to the evaporator only depending on its self-weight.

The only requirement for this to be possible is that the evaporator section must be located below the condenser. The working principle is shown in the figure below.

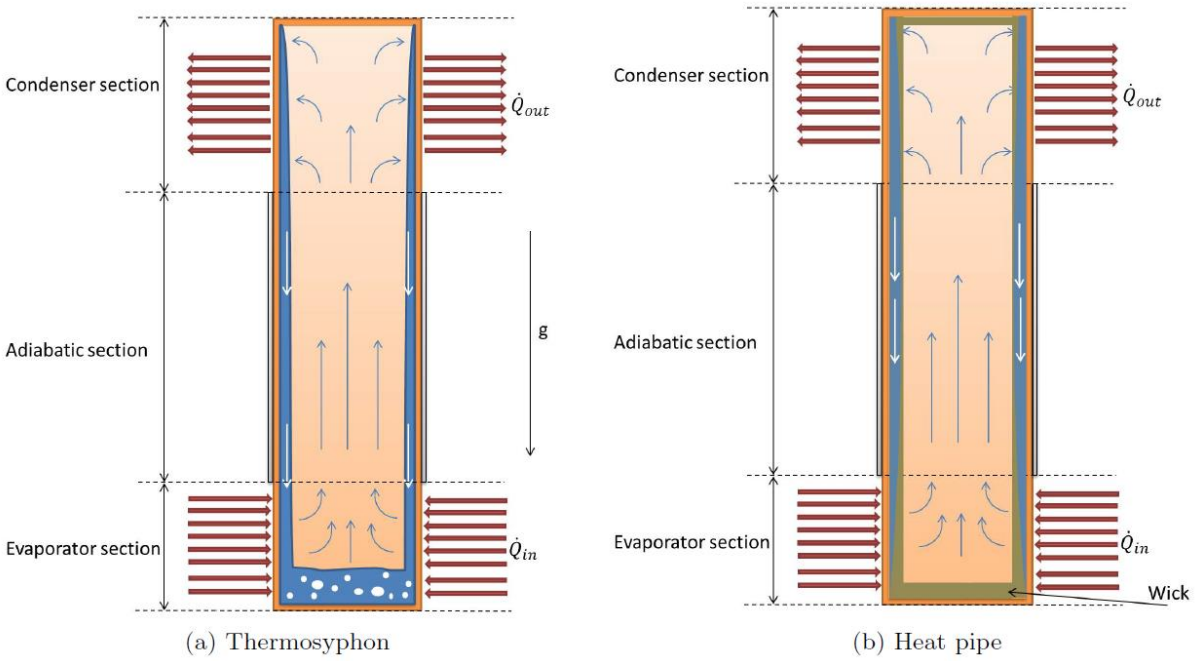

FIGURE 1: WORKING PRINCIPLE OF BOTH THERMOSYPHONS (LEFT) AND CAPILLARY DRIVEN HEAT PIPES (RIGHT).

2.3 Wick structure profiles

Wick structures come in many profiles and configurations depending on the type of heat pipe, working fluid and the operating conditions of the system. These structures are located along the pipe wall and its purpose is to return liquid to the evaporator. One can distinguish between homogeneous and composite wicks. The most important properties for wick structures are:

- Permeability: as high as possible to ensure flow.
- Thermal conductivity: preferably as high as possible to reduce the temperature drop/increase over the heat pipe.
- Minimum capillary pore radius: depending on the capillary forces needed to circulate fluids through the system.

Homogenous wick structures are the simplest types of wicks with respects to machining and costs. The most common types are screens which are pre-machined and inserted into the heat

pipe during installation. Another configuration is sintered metal wick. This wick structure utilizes small metal particles that are pressed together so that they form a porous medium that can be inserted in the heat pipe. Other types will include wicks that are basically solid pieces of metal with various extruded patterns in the bulk such as axial grooves (see figure).

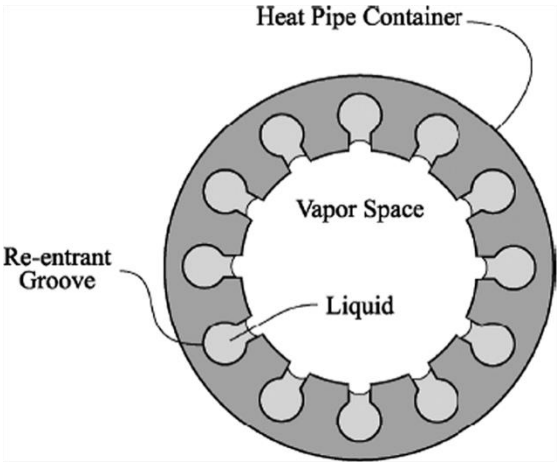

FIGURE 2: HEAT PIPE CROSS SECTION WITH A WICK STRUCTURE MADE OUT BY AXIAL GROOVES TO BETTER ENSURE FLOW AND WETTING OF PIPE WALL.

Composite wick structures are a bit more complex than homogenous types. Like the homogenous types, the simplest is the composite screen wick. This type consists of two different screen layers with different properties in terms of permeability and pore size.

2.4 Heat transfer limitations in heat pipes

Faghri (2014) [11] summarized the various scenarios that may compromise heat transfer in heat pipe operations:

2.4.1 Flooding limit

This is the most common concern in long heat pipe systems. When talking about flooding, the shear forces between the condensed liquid and the travelling vapor creates a hold-up along the heat pipe wall. This film instability results in variable returns of condensed liquid.

The flooding limit in vertical thermosyphons can be calculated by a modified Wallis flooding correlation developed by Sakhuja (1973) [12]:

$$\dot{Q}_{max} = {c_w}^2 \frac{\pi {D_i}^{2,5}}{4} * \frac{r\sqrt{g\,\rho_v\,(\rho_l - \rho_v)}}{[1 + (\rho_v/\rho_l)^{0,25}]^2}$$

The flow coefficient c_w = 0,725, while ρ_v and ρ_l denotes densities for vapor and liquid phase respectively. The equation describes the maximum heat transfer rates one can have before flooding problems will occur.

2.4.2 Entrainment limit

Happens when the radial heat flux in the evaporator becomes too large. Shear forces in the liquid-vapor interface will make the liquid in the wick structure evaporate and the pipe will experience a turn-around in flow direction within the wick. The result of this also concerns the rate of returns to the evaporator end. Eventually, the evaporator may dry completely out.

2.4.3 Capillary limit

Affects the wicks capability of pumping fluid. It is also referred to as capillary limitation or hydrodynamic limitation, and occurs then the pumping rate is not sufficient. Depending on the properties of the wick structure, if the sum of vapor and liquid pressure exceeds the maximum capillary pressure of the wick, you may encounter dry outs in the evaporator section. In such case, it happens because the rate of refill is too low.

2.4.4 Sonic limit

This is a choked flow scenario where the vapor velocity exiting the evaporator section cannot exceed the local speed of sound. Sonic limitation is not considered to be a major failure mode in heat pipe operations, but will to some extent affect the overall heat pipe energy transfer. This happens normally during start-up and will cease to exist when the bottom temperature in the evaporator rises.

2.4.5 Boiling limit

If the radial heat fluxes around the evaporator wall is too large, the liquid in the wick structure will start to form bubbles. These bubbles will prevent the liquid from wetting the wall which again will create hot spots at the evaporator wall. These may eventually lead to burn out in the evaporator section and create further thermal blockage of liquid returns from the condenser section of the pipe.

2.3.6 Vapor pressure limit

In long heat pipes, or in heat pipes with temperatures below the working fluids optimal range, a pressure drop along the center axis of the pipe may occur. In this case, the pressure in the condenser section is nearly zero leading to poor heat and mass transfer.

2.4.7 Condenser heat transfer limit

The condenser makes the cooling part of the heat pipe. If the condenser is not designed properly, the maximum thermal transport capacity can be limited. This applies especially for cases with very high temperatures and often in combination with formation of non-condensable gases.

2.5 Heat pipes applications

The first heat pipe devices were developed by NASA in the 1960s with a purpose to transfer heat from inside space shuttle components to the outside of the shuttle [13]. However, this turned out to be difficult since heat transfer by conduction in vacuum is relatively poor. The idea was that heat was easier to transfer via convection (movement of molecules) rather than conduction (contact between two/several surfaces) and NASA came up with a heat pipe device to serve as cooling units. This has led to a development of heat pipes serving as cooling units not only for space shuttle purposes, but also as smaller scale cooling units such as for processors in personal computers and other electronic systems [10].

2.6 Selecting the right fluid

When searching for a suitable working fluid, one wants a fluid that evaporates at a given temperature, takes up heat and releases the heat again due to the condensation process that occur in the cold section of the heat pipe. Normally one would look at various fluids triple point and phase diagram to determine if the fluid is suitable or not. By looking at this, we get an understanding of when phase changes will take place and under what circumstances.

In addition, one should compare this to the operational requirements of the heat pipe system. The temperature range of the system will dictate if the proposed fluid can be used or not. Heat pipe systems should have an operational temperature range from below the ambient local temperature and up to above the record high [14]. In the case study later in this thesis ammonia is chosen as working fluid.

One should also investigate if the chosen fluid is compatible with the heat pipe wall material. Below is a table with selected potential heat pipe fluids for various conditions.

Working fluid	Boiling point, °K	Useful working range, °K
Ammonia	239,9	213-373
Acetone	329,4	273-393
Water	373,15	303-550
Methanol	337,8	283-403
Freon 11	296,8	233-393

TABLE 1: VARIOUS WORKING FLUIDS

When looking at the table above, it is easy to see that ammonia sticks out as a good fluid for heat pipe applications. In addition to have a useful range of 160 °K, the latent heat of vaporization is also greater than the other fluids in this range. The latent heat of vaporization (heat transmitted to a fluid to undergo a phase change) is 1369 kJ/kg for ammonia at atmospheric pressure which is significantly higher than water. The high latent heat of vaporization allows the ammonia to carry more energy. [11].

3 The thermodynamic cycle of heat pipe systems

3.1 Introducing thermal resistances

Zuo and Faghri [15] described the thermodynamic principle of a basic heat pipe consisting of an evaporator section connected with a condenser section with a wick wall structure. This analysis describes the heat pipe as a network of thermal resistances, where each individual process in the pipe is represented by a thermal resistance.

The different processes are explained as followed:

(1) Radial heat conduction through the evaporator wall
(2) Radial heat conduction through the wick structure in the evaporator end
(3) Vapor flow
(4) Axial heat conduction through the adiabatic section wall
(5) Axial heat conduction through the adiabatic section liquid-wick
(6) Liquid flow
(7) Radial heat conduction through the condenser wick structure
(8) Radial heat conduction through the condenser pipe wall

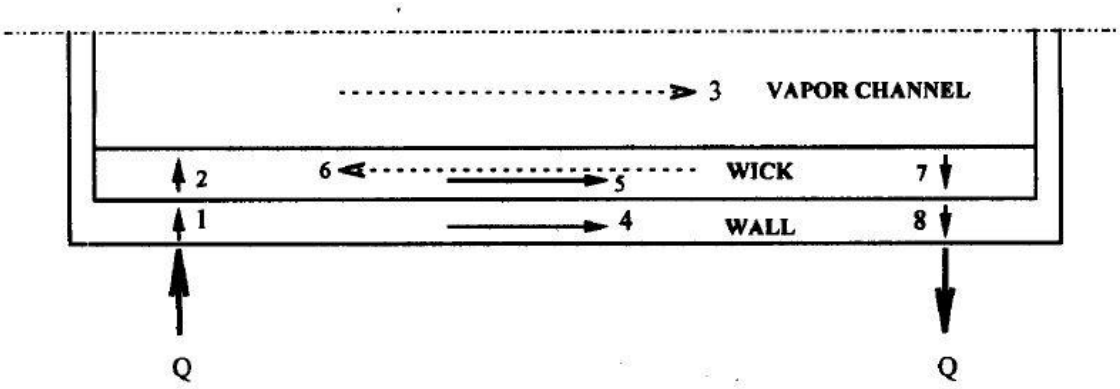

FIGURE 3: HEAT PIPE CROSS SECTION WITH FLUID PROCESSES.

Each process can be described by the following expression:

$$\frac{dT_i}{dt} = \frac{2\alpha_i}{\lambda_i^2}\left(T_{i,1} + T_{i,2} - 2T_i\right)$$

This expression describes the temperature change over a component in the system given an assumption of a temperature T_i in the middle of the specified component, i. The hot and cold side of the system process is denoted as $T_{i,1}$ and $T_{i,2}$ respectively and λ_i is a measure of component thickness. The α is an expression for the components thermal diffusivity which is given by:

$$\alpha_i = \frac{k_i}{A_i \rho_i c_p}$$

Zou and Faghri (1997) used this to develop a model predicting the temperature in each component. Below is a figure of the network overview of resistances followed by a set of equations that can be applied for each component. Note that heat transfer effects by vapor and liquid flow through the adiabatic walls are neglected.

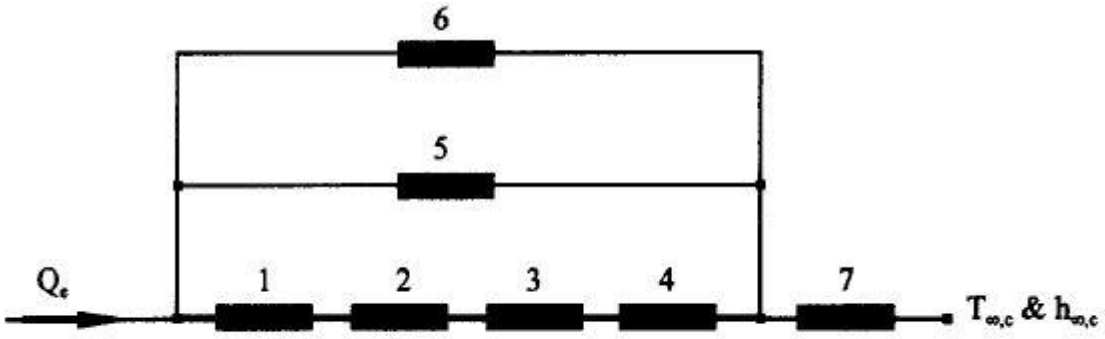

FIGURE 4: HEAT PIPE COMPONENT OVERVIEW.

Each component in the system is classified as:

Q_e: Evaporator heat input

(1) Evaporator wall
(2) Evaporator wick
(3) Condenser wick
(4) Condenser wall
(5) Adiabatic wick
(6) Adiabatic wall
(7) Convective cooling condition (condenser surface outer conditions)

The model is based on the first equation and the two following rules: for each component yields heat input equals heat output, and components exposed to the same temperature will experience the same temperature at corresponding ends. The system can then be described by:

$$\frac{dT_1}{dt} = \frac{2\alpha_1}{\lambda_1^2}[(\varsigma_{1\,2} + \eta_1 - 2)T_1 + \varsigma_{2\,1}T_2 + \eta_5 T_5 + \eta_6 T_6)] + \frac{2\alpha_1}{\lambda_1^2}\frac{Q_e/_2}{k_1A_1/\lambda_1 + k_5A_5/\lambda_5 + k_6A_6/\lambda_6}$$

$$\frac{dT_2}{dt} = \frac{2\alpha_2}{\lambda_2^2}[\varsigma_{1\,2}T_1 + (\varsigma_{2\,1} + \varsigma_{2\,3} + 2)T_2 + \varsigma_{3\,2}T_3]$$

$$\frac{dT_3}{dt} = \frac{2\alpha_3}{\lambda_3^2}[\varsigma_{2\,3}T_2 + (\varsigma_{3\,2} + \varsigma_{3\,4} + 2)T_3 + \varsigma_{4\,3}T_4]$$

$$\frac{dT_4}{dt} = \frac{2\alpha_4}{\lambda_4^2}[\varsigma_{4\,3}T_3 + (\varsigma_{4\,3} + \eta_4 - 2)T_4 + \acute{\eta}_5 T_5 + \acute{\eta}_6 T_6)] + \frac{2\alpha_4}{\lambda_4^2}\frac{h_{\infty,c}S_cT_{\infty,c}/_2}{k_4A_4/\lambda_4 + k_5A_5/\lambda_5 + k_6A_6/\lambda_6 + h_{\infty,c}\,S_c/2}$$

$$\frac{dT_5}{dt} = \frac{2\alpha_5}{\lambda_5^2}[\eta_1 T_1 + \acute{\eta}_4 T_4 + (\eta_5 + \acute{\eta}_5 - 2)T_5 + (\eta_6\acute{\eta}_6)T_6)] + \frac{2\alpha_5}{\lambda_5^2}\frac{Q_e/_2}{k_1A_1/\lambda_1 + k_5A_5/\lambda_5 + k_6A_6/\lambda_6} + \frac{2\alpha_5}{\lambda_5^2}\frac{h_{\infty,c}S_cT_{\infty,c}/_2}{k_4A_4/\lambda_4 + k_5A_5/\lambda_5 + k_6A_6/\lambda_6 + h_{\infty,c}\,S_c/2}$$

$$\frac{dT_6}{dt} = \frac{2\alpha_6}{\lambda_6^2}[\eta_1 T_1 + \acute{\eta}_4 T_4 + (\eta_5 + \acute{\eta}_5)T_5 + (\eta_6 + \acute{\eta}_6 - 2)T_6)]$$

$$+ \frac{2\alpha_6}{\lambda_6^2} \frac{{Q_e}/{2}}{k_1 A_1/\lambda_1 + k_5 A_5/\lambda_5 + k_6 A_6/\lambda_6}$$

$$+ \frac{2\alpha_6}{\lambda_6^2} \frac{{h_{\infty,c} S_c T_{\infty,c}}/{2}}{k_4 A_4/\lambda_4 + k_5 A_5/\lambda_5 + k_6 A_6/\lambda_6 + h_{\infty,c}\, S_c/2}$$

The different factors η, ή and ς are given by:

$$\varsigma_{i\,j} = \frac{{k_i A_i}/{\lambda_1}}{{k_i A_i}/{\lambda_i} + {k_j A_j}/{\lambda_j}}$$

$$\eta_i = \frac{{k_i A_i}/{\lambda_1}}{{k_1 A_1}/{\lambda_1} + {k_5 A_5}/{\lambda_5} + {k_6 A_6}/{\lambda_6}}$$

$$\acute{\eta}_i = \frac{{k_i A_i}/{\lambda_i}}{k_4 A_4/\lambda_4 + k_5 A_5/\lambda_5 + k_6 A_6/\lambda_6 + h_{\infty,c}\, S_c/2}$$

These equations describing T_1 through T_6 are first order differential equations and can be solved by using fourth order Runge-Kutta method.

3.2 Working fluid dynamics

As the energy carrier, the working fluid must be in circulation at all time during operation of the heat pipe. Throughout the thermodynamic cycle, the working fluid will experience four different processes. These processes will then represent the different states the working fluid is in. As shown above, the heat pipe operation can be shown as a network of thermal

resistances, but it can also be represented by a T-s diagram showing the different states of the working fluid [15].

The different states are:

- A: Subcooled liquid in the evaporator
- B: Vapor in the evaporator
- C: Vapor in the condenser
- D: Subcooled liquid in the condenser

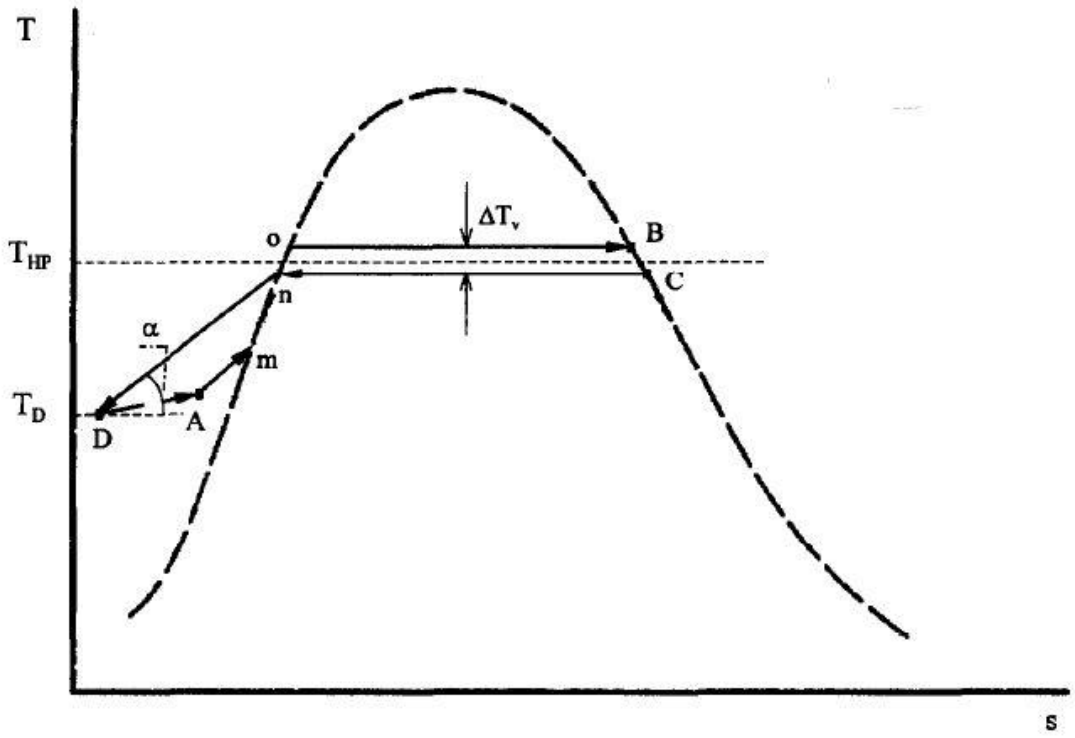

FIGURE 5: T-S DIAGRAM SHOWING THE DIFFERENT STATES OF THE WORKING FLUID.

For the fluid to inhabit a certain state (A-D), a process equivalent to the change of state can be specified. The working fluid cycle is shown in the diagram above.

A → B: Heat from the source heats the working fluid and raises the internal energy and entropy. At state B, the working fluid is turned into vapor.

B → C: The newly formed vapor travels way from the evaporator section and into the condenser section in opposite end of the pipe.

C → D: The working fluid releases its latent heat energy and undergoes a phase change into liquid in the condenser.

D → A: the condenser liquid travels back to the evaporator.

Based on this, Zou and Faghri (1997) describe the following energy balance employing a classical thermodynamic approach of applying the first law of thermos dynamics: principle of conservation of energy.

This law states that the total amount of energy in a closed and isolated system is constant. A maybe better definition is that the total internal energy of a system is equal to the heat applied to the system from an outside source, minus the work done by the system and heat rejected from the system [9]. This leads to the following balance:

$$Q_{A-B} = W_{B-C} + Q_{C-D} + W_{D-A} = 0$$

or

$$Q_{out} = W_{B-C} + Q_{C-D} + W_{D-A}$$

From this energy balance, one can define the amount of heat applied/rejected to the system and the work done by the system from the following equations presented by Zuo and Faghri (1997):

Energy applied to the system changing the working fluid state from A to B:

$$Q_{A-B} = m(h'_B - h'_A)$$

Work done by the working fluid by travelling from B to C is mainly caused by friction between the travelling vapor and the pipe wall:

$$m(h'_C - h'_B) = W_{B-C} = \frac{m}{\rho_v}(P_{v\,C} - P_{v\,B})$$

The systems heat rejection and phase change from vapor to liquid can be expressed as:

$$Q_{C-D} = m(h'_D - h'_C)$$

Liquid returns to the evaporator section either by gravity or assisted by a wick structure:

$$m(h'_A - h'_D) = W_{D-A} = \frac{m}{\rho_l}(P_{l\,A} - P_{l\,D})$$

As for the travelling vapor, a small increase in temperature and entropy can be spotted on T-s diagram when the liquid travels from the condenser and back to the evaporator. This is also caused by contact friction between the liquid and the pipe wall.

Zou and Faghri (1997) then describes how to apply the network model presented to determine the various fluid states (A, B, C and D) in the cycle. To do this, one can follow three steps:

Step 1: determine the pressure difference from fluid state B to C.

$$\Delta P_{B\to C} = \frac{8Q\mu_v}{\pi\rho_v h_{fg} R_v^4}(0{,}5L_e + L_a + 0{,}5L_c)$$

The variable R_v is defined as the radius of the vapor flow channel and if a non-circular area is used for the heat pipe system, a hydraulic radius will work. The heat pipe operating temperature is defined as T_{HP} and relates to the vapor temperature when travelling from evaporator to condenser.

If the pressure difference is obtained and one assume that the working fluid is saturated vapor in state B and C, temperature T_B and T_c may be found by solving the following equations:

$$T_B = T_{HP} + \frac{1}{2}\Delta T_v, \qquad T_C = T_{HP} - \frac{1}{2}\Delta T_v$$

Step 2: State D relates to the pressure and temperature in the condenser section. For most applications, this will be a given parameter based on the outside conditions and thus simple to obtain.

Step 3: Defining the properties of state A. The pressure difference between the liquid in the condenser and the liquid that have traveled to the evaporator can be found by:

$$\Delta P_{D\to A} = \frac{\mu_l m_l}{\rho_l A_w K} L_a$$

K denotes the wick permeability and A_w defines the cross-sectional area of the wick structure. In this thesis, how to find the temperature in state A will not be shown. The temperature in A can be approximated to the temperature in D, but another possibility is shown by Zou and Faghri (1997) in their presentation of the network model.

Now, one has obtained the pressure and temperature in every state which lets us determine the entropy and enthalpy changes as well as work done by every process. This may be useful information when designing heat pipes or if it is desirable to know more specifics about different processes in the cycle.

One should note that this model is intended for heat pipes applying wick structures and not for pipes with smooth wall surfaces.

4 Bridge deck experiments

The following heat transfer model is developed by heat pipe experiments executed on two test facilities and the explanation that follows is taken from reports made by Nydahl et. al [14, 16].

The first system was built in 1974 near Sybille Canyon in Wyoming, featuring 12 heat pipes with evaporator lengths of 12 meters heating an 11 m^2 test surface. The second facility was built in Spring Creek in 1980. The Spring Creek facility featured a much larger system than Sybille Canyon and 15 heat pipes were installed in each corner of a bridge surface (a total of 60 heat pipes). The vertical evaporator lengths were 30,5 m and the condenser sections reached from 12,5 m to 6,4 m into the concrete deck (see appendix C for detailed schematics). Ammonia was chosen to be the working fluid in both projects [14].

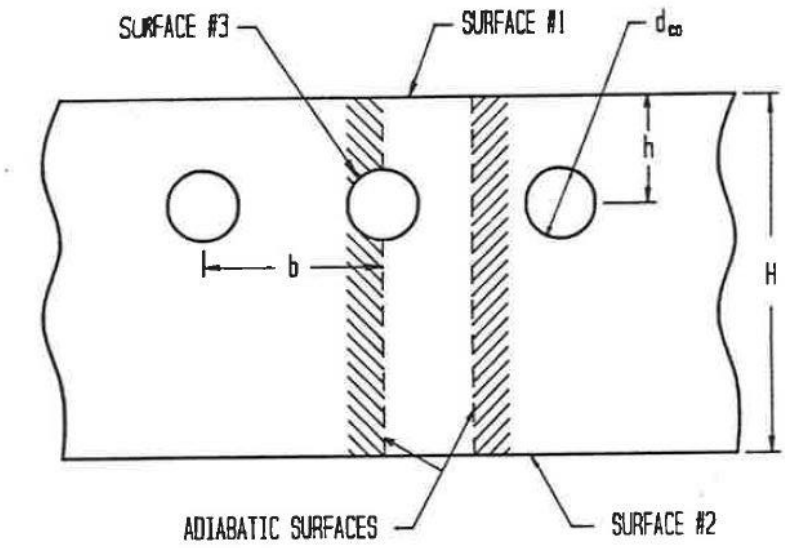

FIGURE 6: SURFACE DESIGNATION IN THE TOP CONCRETE SEGMENT OF THE HEAT PIPE SYSTEM INCLUDING CONDENSER SURFACE #2 AND BRIDGE DECK TOP AND BOTTOM AS #1 AND #3 RESPECTIVELY.

The model developed by Nydahl et. al (1986) consists of four equations describing the heat that have passed through different surface layers in the system (see figure 6). This together with the additional heat provided by solar radiation and air temperature give the following set of equations.

(1) Top deck surface temperature, $T_{1,0}$:

$$\sum_{j=1}^{3}\sum_{k=0}^{N} X'_{1jk}\, T_{jk} + CR * q_{1,k} = \alpha_{sw} q_{solar} + \alpha_{lw}\varepsilon_{air}\sigma T_{air}^4$$

(2) Bottom deck surface temperature, $T_{2,0}$:

$$\sum_{j=1}^{3}\sum_{k=0}^{N} X'_{2jk}\, T_{jk} + CR * q_{2,k} = -u_{insul}(T_{2,0} - T_{air})$$

(3) Condenser pipe inner surface temperature, $T_{3,0}$:

$$\sum_{j=1}^{3}\sum_{k=0}^{N} X'_{3jk}\, T_{jk} + CR * \quad \dot{Q}_{3,1}/A_{cond} = \quad \dot{Q}_{3,0}/A_{cond}$$

(4) Heat pipe power, $\dot{Q}_{3,0}$:

$$T_{3,0} = -R_{hp} * \dot{Q}_{3,0} - \sum_{j=1}^{N}\sum_{k=0}^{\infty} W_{ijk}\, \dot{Q}_{3,k} + T_g$$

- R_{hp} is defined as the heat pipe thermal resistance:

$$R_{hp} = \frac{\ln(\frac{d_{eo}}{d_{ei}})}{2\pi K_e\, l_p} + \frac{\ln(\frac{d_{co}}{d_{ci}})}{2\pi K_c\, l_c} + \frac{1}{\pi d_{ei} l_p h_e} + \frac{1}{\pi d_{ci} l_c h_c}$$

Notable features with this model are that k denotes the number of time steps back in time from present (k=0) and T denotes the temperature at surface number j at timestep k.

5 Case introduction and methodology

In the light of available methods found in the literature [14, 15], a theoretical case can be performed by adjusting the models to a Norwegian environment and see if a similar system can be utilized with a beneficiary outcome. The first thing that needs to be done is to develop a model that will predict the heat flow through the given system. The system is then assumed to deliver heat during a period of time. Once this is done, there will be an estimate of the cost of the system followed by an evaluation of profitability based on the net present value method.

5.1 Case model and system overview

The system that is evaluated is a gravity assisted heat pipe with no wick structure (thermosyphon) installed in a well. The well is drilled by a mobile drilling rig similar to those that drill geothermal heat pumps and water wells. After the well is drilled and the heat pipe is inserted, the annulus along the evaporator wall is filled with thermal grout or some sort of backfill to ensure good contact between evaporator and formation.

Parts of the heat transfer model developed from the test facilities in Sybille and Spring Creek [16] will be used to determine the heat transfer. The maximal energy output delivered from this system can be express by the following design equation:

$$Q_{thermal} = u_{system}(T_{ground} - T_{surface})$$

As the energy balance above implies, the system will be expressed by a value of thermal conductance. This value will be estimated by splitting the system into smaller components and consider each of the components as a surface that transmits heat. To better understand the approach that is chosen, one can consider some basic thermodynamic equations which are explained with reference to the figure depicted on the next page.

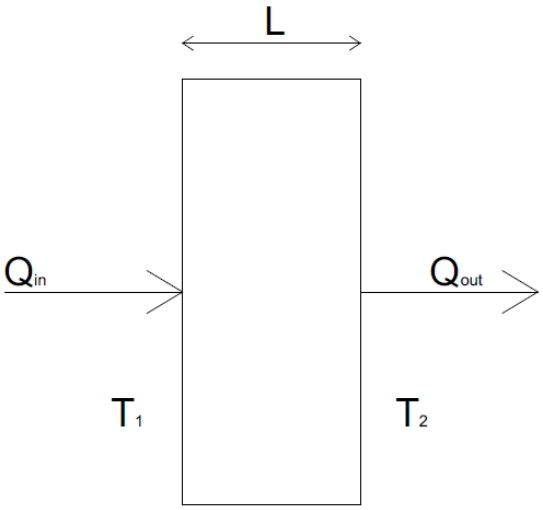

FIGURE 7: HEAT FLOW THROUGH AN ARBITRARY OBJECT WALL.

The first equation is an expression for thermal conductivity where heat denoted as q is transmitted through the surface of a specimen with a thickness of L. Note that the unit of q in this case is W/m^2 .

$$k = q\frac{L}{\Delta T}$$

From this, it is possible to express the thermal resistance of an object. To transfer heat between the walls of an object, there needs to be a temperature difference across the walls. This equation is a measure for how much the temperature will increase/decrease in unit temperature per unit of heat supplied to the system. The unit of thermal resistance is m^2 K/W.

$$R = \frac{\Delta T}{q} = \frac{L}{k}$$

If the two equations above are combined, the total thermal conductance of a specimen can be written as below.

$$U = \frac{q}{\Delta T} = \frac{1}{R} = \frac{k}{L}$$

The thermal conductance expresses the ability of a surface of an object to transfer heat across the border walls. This in mind, we can express the thermal conductance of the system as the following equation.

$$Q_{thermal} = U_{system} * \Delta T = \frac{1}{R_{system}} * \Delta T$$

If the system is considered as a series of thermal resistances, the total thermal resistance can be found by a summation of all individual resistances. The same yields for thermal conductance, and by defining each of the resistances in the heat pipe the following figure can be used to express the system thermal layout.

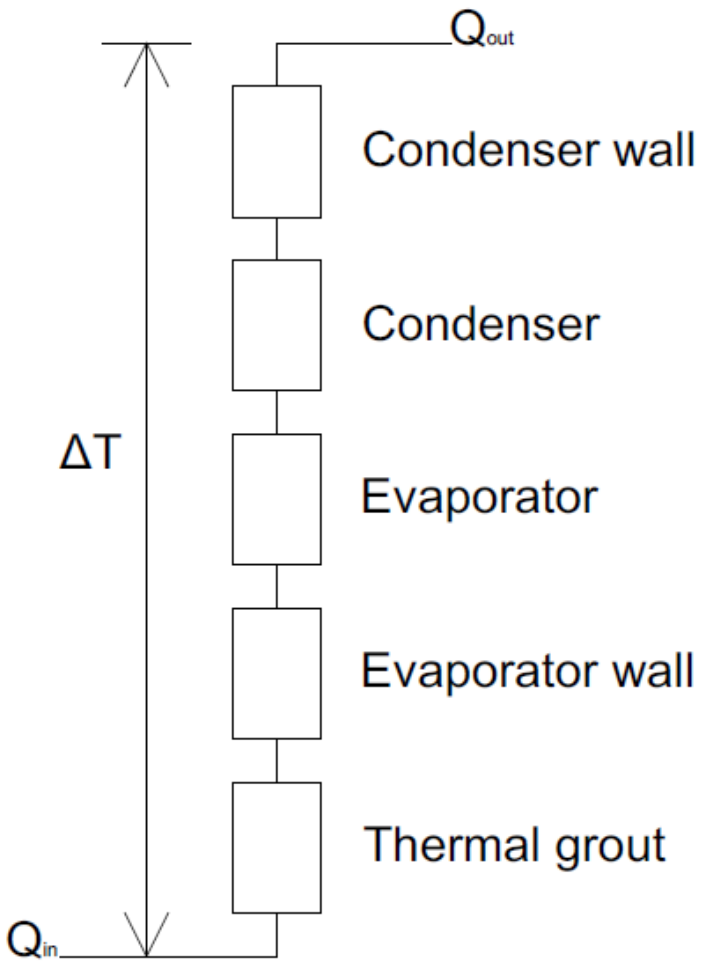

FIGURE 8: OVERVIEW OF SYSTEM COMPONENTS.

As this overview is established, it is possible to write the following summation of system components to determine the thermal conductivity based on the thermal resistances in the system.

$$R_{System} = R_{Thermal\ grout} + R_{evap.\ wall} + R_{evap.} + R_{Cond.} + R_{Cond.\ wall}$$

$$R_{Evap.\ wall} = \frac{\ln(^{d_{eo}}/_{d_{ei}})}{2\pi\ K_e\ l_e}$$

$$R_{Evap.} = \frac{1}{\pi\ d_{ei}\ h_e\ l_e}$$

$$R_{Cond.} = \frac{1}{\pi\ d_{ci}\ h_c\ l_c}$$

$$R_{Cond.\ wall} = \frac{\ln(^{d_{co}}/_{d_{ci}})}{2\pi\ K_c\ l_c}$$

$$R_{Thermal\ grout} = \frac{\ln(^{d_{well}}/_{d_{eo}})}{2\pi\ K_{grout}\ l_e}$$

The expression itself is telling us how much the temperature will change from the contact between the formation and thermal grout to the outside of the condenser walls. Note that heat transfer through evaporation and condensing of the working fluid is denoted as h_e and h_c respectively. These heat transfer coefficients represent fluid film coefficients and will be addressed more in detail in the discussion later in the thesis.

$$R_{system} = \frac{\ln(^{d_{well}}/_{d_{eo}})}{2\pi\ K_{grout}\ l_e} + \frac{1}{\pi\ d_{ei}\ h_e\ l_e} + \frac{\ln(^{d_{eo}}/_{d_{ei}})}{2\pi\ K_e\ l_e} + \frac{\ln(^{d_{co}}/_{d_{ci}})}{2\pi\ K_c\ l_c} + \frac{1}{\pi\ d_{ci}\ h_c\ l_c}$$

For this approach to be valid, the following Assumptions for the heat transfer method are made:

- Steady state conditions.
- The heat transfer through the heat pipe is to be considered as a stationary process.
- Uniform ground temperature equivalent to the local geothermal gradient.
- Isothermal properties subsurface rocks.
- The pipe section between evaporator and condenser is to be considered adiabatic.
- The heat pipe is connected to a heat exchanger which has an efficiency of 50 %.
- Heat exchanger and surface delivery pipe infrastructure are already in place.

5.2 Case economics

When investigating profitability for this system, the chosen method is the net present value method. This method sums the annual cash flow throughout the life time of the project and is a common method to use in hydropower projects [17]. The net present value is given by the following equation:

$$Net\ present\ value = \sum_{t=0}^{N} \frac{R_t}{(1+i)^t}$$

$$R_t = cash\ flow\ in\ year\ t$$

$$i = Bank\ rate$$

$$t = year\ number$$

$$N = system\ life\ span$$

Since this is a system that does not produce any electric power, the cash flow in this case will be assumed to be money saved by the consumer. The money that is saved will be based on how much electric power that is not used for heating purposes.

As stated in the introduction to this thesis, almost 50 % of all consumed energy in Norway is electricity, of which 85 % to 90 % is used for heating. This gives a total potential of 94 TWh of electricity to be saved in the consumer market. The total cash flow will be equal to the energy delivered by a heat exchanger standing top side and the energy supplied to the heat exchanger will come from the heat pipe system.

The bank rate is a measure of how much interest the investors will see annually if the income from an investment is transferred to a bank. In this case, the income is the money that are saved by the consumer, meaning that there is no real income. Therefore, an assumption is made that all money saved during the systems life span is put in the bank and the bank rate will relate to this money instead. The rate used for this case exercise is 3,5 % and is a rate that is recommended in when planning small hydropower projects. Total life span of the project is 30 years and price is assumed to be 1 NOK/kWh with all fees included [18].

5.3 Cost drivers

5.3.1 Transportation of equipment and site preparation

Transportation of equipment such as drilling rig, pump systems etc. is estimated to cost 10.000 NOK. This value also includes preparations needed to start up drilling of the well. The cost is based on industry practice [19].

5.3.2 Drilling the well

When estimating the cost of drilling the well a value of 1000 NOK/meter is used. This value is taken from a similar project in the Oslo area [20] where a geothermal heat pump was installed at 800 meters of depth. Drilling the well with this price assumes no significant problems during this phase. The cost for backfill at the evaporator end is neglected.

5.3.3 Pipe material

The heat pipe system will be made of steel pipes with a fixed diameter along the well. The price for a typical welded steel pipe is 221,7 NOK/meter [21].

5.4.4 Working fluid

The working fluid is chosen to be ammonia. The price for liquid ammonia in 2017 is 35 NOK/liter. This value is given to the author through an e-mail correspondence with Air Liquide Norway AS.

5.5.5 On site assembly of heat pipe and installment

After the well is drilled, the pipe needs to be inserted into the well. Each of the pipe segments of 6 meter need to be welded together and pressure tested to ensure that there is no leakage in the system. A cost of 100 NOK/meter is estimated based on industry practices.

5.5.6 Maintenance

A maintenance cost of 10.000 NOK/year is estimated to be adequate for system check and change of working fluid if necessary. Maintenance will also cover evacuation of non-condensable gases.

5.6 System parameters

As assumed previously in this thesis, the ground temperature follows a geothermal gradient equal to 0,02 °C/m. The surface temperature is assumed to be the local average temperature at Florida meteorological station in Bergen, Norway [22]. The following table shows the monthly average temperature at this station.

Month	Monthly average (°C)	Normal average (°C)
April 2017	6,2	5,9
Mars 2017	4,7	3,3
February 2017	3,0	1,5
January 2017	3,6	1,3
December 2016	6,1	2,4
November 2016	4,0	4,6
October 2016	8,3	8,6
September 2016	15,2	11,2
August 2016	14,2	14,1
July 2016	14,7	14,3

June 2016	15,3	13,3
May 2016	12,2	10,5
April 2016	6,2	5,9

TABLE 2: MONTHLY TEMPERATURE DISTRIBUTION FROM FLORIDA METEOROLOGICAL STATION, BERGEN.

The parameters for the well and the heat pipe system are largely based on what the technology is capable of today. The borehole is assumed to have a diameter of 12 cm, and constraints for the heat pipe insertion are chosen to be 1 inch radial clearance.

5.6.1 Evaporator parameters

Element	Value	Unit
d_{eo}	0,070	m
d_{ei}	0,0691	m
l_e	30	m
K_e	45	$\frac{W}{m * K}$
h_e	2040	$\frac{W}{m^2 * K}$
$R_{evaporator\ section}$	$7{,}679 * 10^{-5}$	$\frac{K}{W}$

TABLE 3: EVARPORATOR PARAMETERS

5.6.2 Condenser parameters:

Element	Value	Unit
d_{co}	0,070	m
d_{ci}	0,0691	m
l_c	30	m
K_c	45	$\frac{W}{m * K}$
h_c	7950	$\frac{W}{m^2 * K}$
$R_{condenser\ section}$	$2{,}0840 * 10^{-5}$	$\frac{K}{W}$

TABLE 4: CONDENSER PARAMETERS

5.6.3 Adiabatic section

Element	Value	Unit
$l_{adiabatic}$	740	m
d_{ao}	0,070	m
d_{ai}	0,0691	m
$R_{adiabatic}$	0	$\frac{K}{W}$

Table 5: Adiabatic pipe parameters

5.6.4 Thermal grout/backfill

Element	Value	Unit
$K_{grout/backfill}$	4	$\frac{W}{m * K}$
d_{well}	0,120	m
d_{eo}	0,070	m
$l_{grout} = l_e$	30	m
$R_{Grout/backfill}$	$7{,}149 * 10^{-4}$	$\frac{K}{W}$

Table 6: Parameters for thermal grout/backfill

5.6.5 Overall system key values

Element	Value	Unit
$R_{Heat\ pipe}$	$9{,}764 * 10^{-5}$	$\frac{K}{W}$
R_{System}	$8{,}125 * 10^{-4}$	$\frac{K}{W}$

Table 7: System key parameter values

6 Results

In this section, there will be a presentation of what we could expect the system to extract in terms of geothermal heat, and there have been made an investigation to see if this system could be profitable if utilized in Norway.

6.1 Production numbers

The graph below shows the maximum theoretical energy output the system can deliver through a heat exchanger with 50 % thermal efficiency during a year of production. The ΔT across the system is based on the temperature table shown in section 5.6 and a constant ground temperature at 800 m TVD of 20 °C. This is done to show how the system will respond to temperature changes during summer and winter seasons during a normal year.

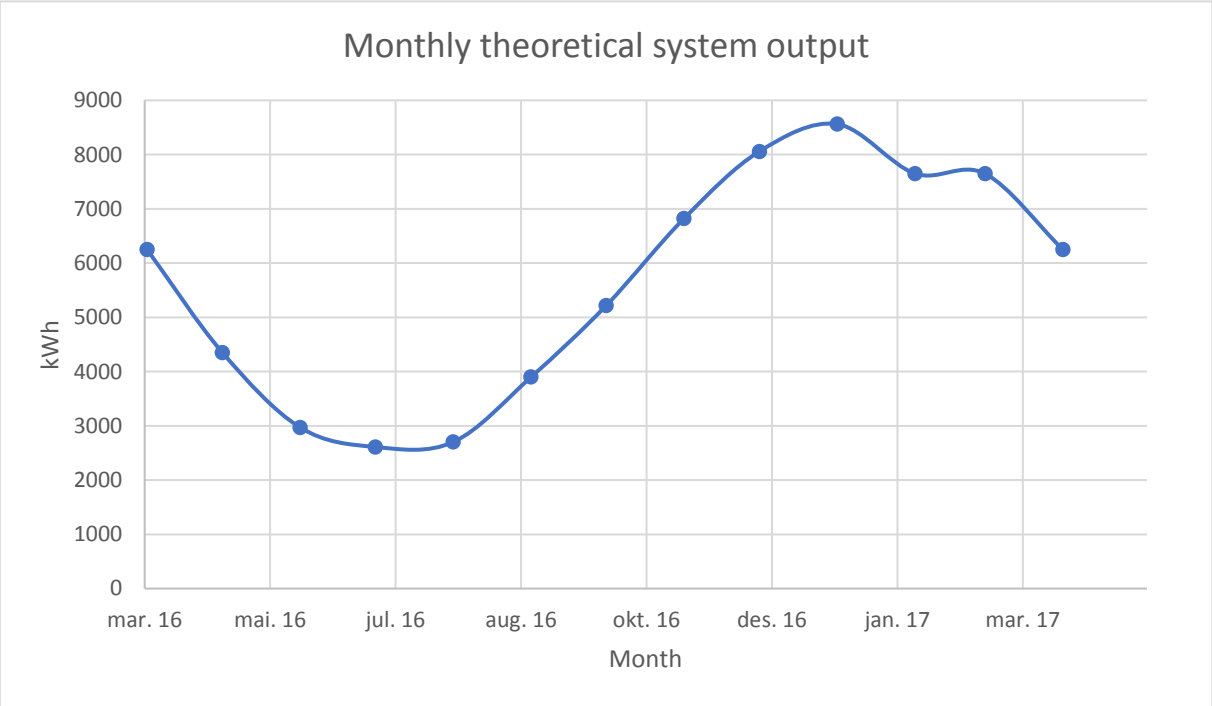

PLOT 1: THEORETICAL EXPECTED ENERGY PRODUCTION DURING A NORMAL YEAR.

From this graphical representation, it is clearly that the fluctuations from winter to summer is severe. The average production per month would be approximately 5600 kWh of extracted thermal energy. This representation also implies that the most profitable period of production

is in the winter season. The month that is likely to produce the least amount of energy is then July with an expected production of 2010 kWh, while the most productive month is January with just short of 8600 kWh.

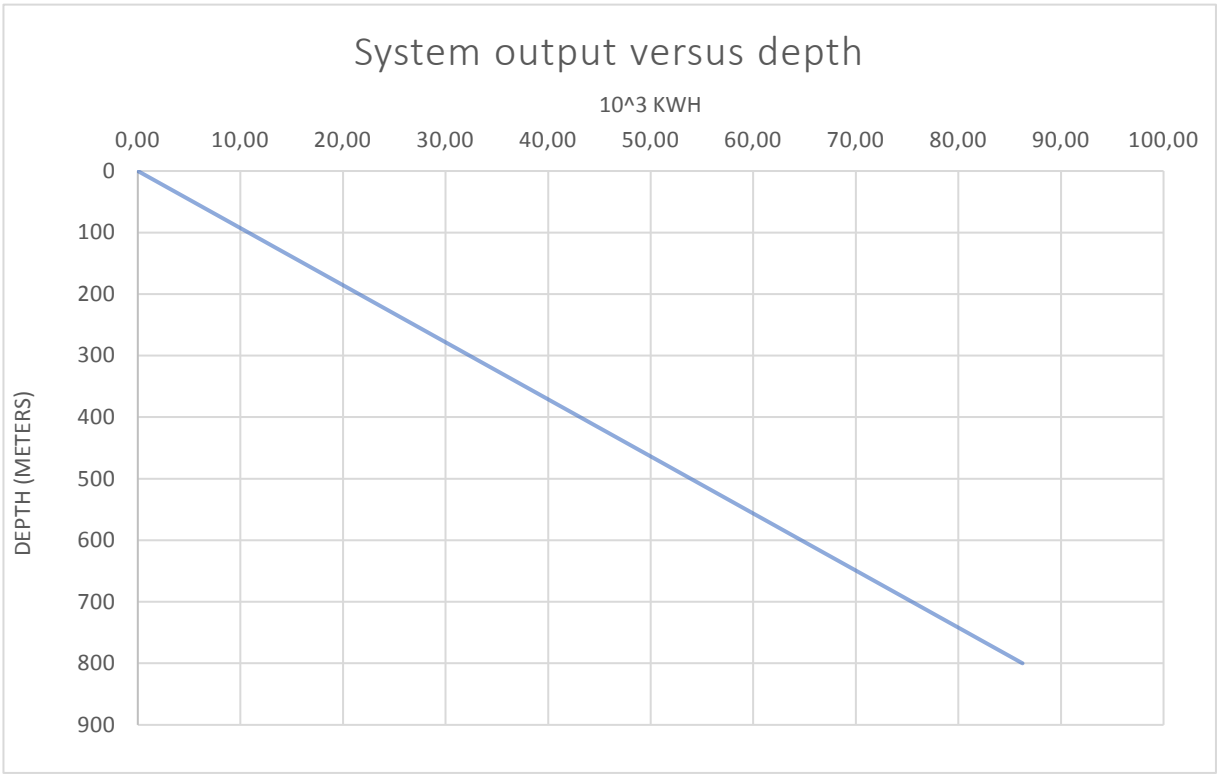

PLOT 2: THERMAL ENERGY PRODUCTION AS A FUNCTION OF DEPTH.

Another feature regarding production is shown by the graph above. This is representation of the system output as a function of depth. The only thing which is changed from the base case is drilled depth. The temperature difference is based on an average surface temperature of 7,45 °C and a ground temperature following the geothermal gradient of 0,02 °C/m. As depicted, the heat pipe power follows the geothermal gradient and is expressed linearly down through the subsurface. A more detailed table of production numbers regarding each individual depth can be viewed in appendix A.

6.2 System costs and net present values

If we look at the cost of this system, the system costs are highly influenced of how deep the well is drilled which leads to how long the installed heat pipe will be. If we consider a base case where the drilled depth is 800 meters, the cost is estimated to be as in the table below.

Bank rate	**3,5%**
Electricity price	1,00 NOK/kWh
Average heat production	86 252,4 kWh/year
Maintenance costs	10 000 NOK/year
Total investment	**1 071 360 NOK**
Cash flow	**70 252 NOK/year**
Net present value	**331 077 NOK**

TABLE 8: BASE CASE KEY VALUES.

As displayed above, the system shows profitability as the net present value is positive. This can be explained with this being a passive system that has very low operating costs. The cash flow is relatively high compared to the investment and there is only one one-time payment which is the system investment itself. The payback time for the base case is 14,1 years, meaning that break-even is reached nearly halfway through the projects life span.

The net present value for a heat pipe system installed at an arbitrary depth is shown below.

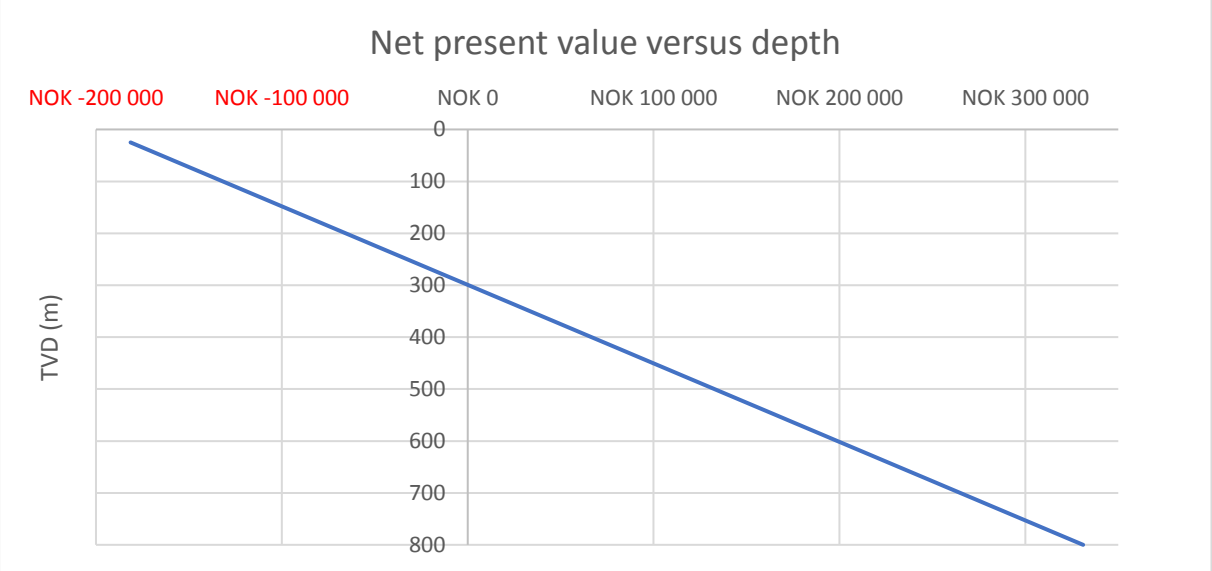

PLOT 3: NET PRESENT VALUE AT AN ARBITRARY DEPTH.

This representation implies that utilization of a heat pipe system should be installed at depths greater than approximately 300 meters. If the system is installed at shallower depths, the cash flow generated from the system would not be enough to reach break-even within the lifetime expectancy of the project.

If we isolate the depth where net present value equals zero, the system would have the following key values based on the analysis performed:

Bank rate	**3,5%**
Electricity price	1,00 NOK/kWh
Average heat production	32 334,64 kWh/year
Maintenance costs	10 000 NOK/year
Total investment	**410 510 NOK**
Cash flow	**22 225 NOK/year**
Net present value	**0 NOK**

TABLE 9: KEY VALUES AT REQUIRED DEPTH TO REACH BREAK-EVEN

6.3 Sensitivity analysis

The sensitivity analysis investigates the change in net present value if key economical parameters are changed.

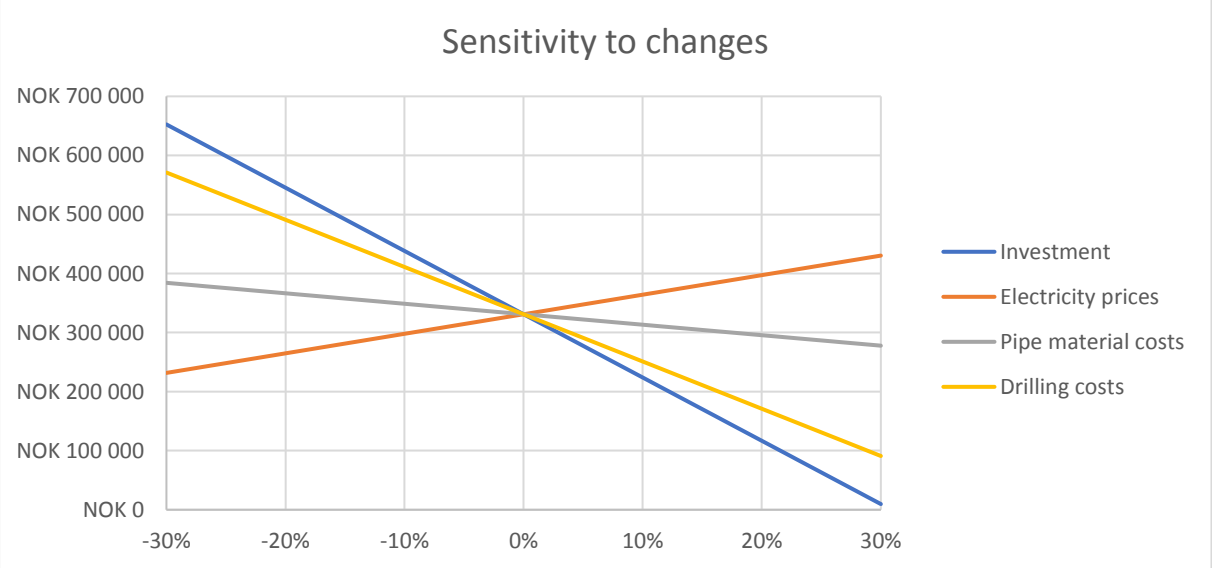

PLOT 4: THE SYSTEM CAPABILITY TO DEAL WITH ECONOMIC CHANGES.

We see from the different slopes that the total investment cost is the biggest threat to the profitability of the base case. Despite this, the base case is still able to handle up to a 30 % increase in investment costs. Another interesting feature is the slope for pipe material. The graph implies that the pipe material is not affecting the net present value in any significant way, but this is up for discussion later in the thesis.

7 Discussion and thoughts around the result

This section will address the results and the methods used during the approach and determination of models and other things relevant.

The first thing to be addressed is one of the initial assumptions stated in the case introduction which make way for a model that consists of an array of thermal resistances. When assuming isothermal properties of the subsurface rocks, the temperature remains constant at the value of what the geothermal gradient estimates it to be. The same yields for heat transfer properties of the rock surrounding the evaporator section of the heat pipe. The problem when assuming this is that one does not take into consideration the possibility of formation cooldown. This meaning, during normal operation the temperature at the surface between the thermal grout/backfill and formation will start to drop. This is relevant because it affects the production numbers in the way that estimated extracted heat from the ground is likely to be significantly lower in real life because of this. However, since this is not an assessment of the rocks' capability to deliver heat, but rather an estimation of the maximum amount of heat that can be extracted by a heat pipe system, the assumption is considered necessary for the developed model to be valid and therefore correct to make.

The second thing that needs explanation is related to the adiabatic pipe section between the evaporator and the condenser. It is assumed that no heat will be exchanged by the travelling vapor and the surrounding elements, as well as no heat delivery from the surroundings to the returning liquids. Especially in long heat pipes, this is an aspect that there exists little research about, and it is thinkable that long adiabatic sections may be influenced by factors mentioned above resulting in poor liquid delivery to the evaporator and reduced vapor energy.

This leads to the heat transfer limitations described in the earlier parts of this thesis. These have not been further discussed and are largely based on experiments executed on small diameter heat pipes. The approach chosen in the case study does not account for the presented limitations which may compromise the overall production rates of heat from the system. The most relevant ones are the flooding, entrainment and sonic limits. For long big-bore heat pipes, it is difficult to make up an opinion whether this would be an issue, especially in systems with relatively long evaporator sections.

Regarding the heat transfer model that is used to determine the heat production, there are some uncertainties related to heat transfer in the evaporator and condenser sections. In the base case, the thermal resistances of the evaporator and condenser sections are determined by utilizing the film coefficients h_e and h_c. The use of these values brings up another issue and that is related to the boiling regime that occurs in the evaporator section of the system. Estimating a value for heat transfer in boiling ammonia is done by correlations and experimental data which provide an empirical value based on the heat added, surface roughness of the boiling area and saturation pressure of the liquid. This is already explained in the literature, and in this thesis, the chosen values for these coefficients are the same as in the bridge deck experiments [14, 16].

If the changes in evaporator and condenser thermal resistances are compared to the heat pipe output power, it is possible to say something about the uncertainties that are connected to this issue. Below is a representation of this.

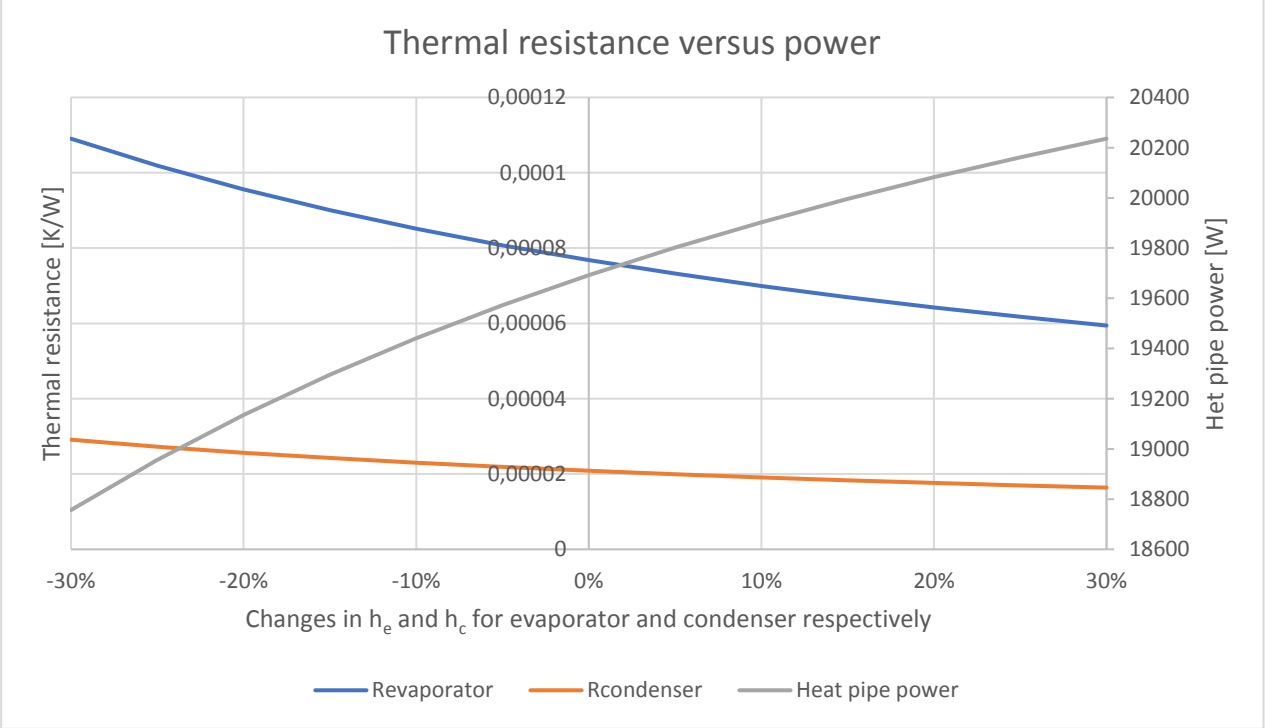

PLOT 5: GRAPHICAL REPRESENTATION OF ELEMENTS IN THE HEAT TRANSFER MODEL. THE HEAT PIPE POWER AXIS REPRESENTS THERMAL ENERGY IN WATTS.

To say something about the accuracy of this model is difficult without relevant test data, but what the graphs above show us is that the influence of a change in values of h_e and h_c does not necessarily affect the heat pipe power so much as one initially would think. A 30 % increase

in film coefficients raises the output power from about 19700 W to 20336 W which implies that other factors in the heat transfer model are more crucial to understand better when estimating the heat pipe power. If we compare the heat pipe resistance to the resistance of the thermal grout/backfill, the thermal resistance of the heat pipe is only 13 % of the resistance element connecting the heat pipe to formation. This shows us that the bottleneck in this equation is not necessarily heat transfer characteristics of the working fluid, but rather the properties of the material chosen to extend the formation into the evaporator section of the pipe.

An issue that is most likely to occur in a heat pipe system extended over 800 meters, is the difficulty of ensuring a wet pipe surface so that returning condensed liquid reaches the evaporator. To the author's knowledge, there has never been built a system that is described in the base case, especially not a system that extends so deep. The bridge deck experiments [14, 16] had vertical sections that were 30 meters and the operation of these pipes indicated no significant problems with liquid returns. If regular steel pipes, like in the base case, turn out to not wet the pipe walls adequately, then a more suitable inside geometry must be used. It is still a very uncertain aspect of the heat pipe operation, and without relevant test data or experiment monitoring data, it is impossible to conclude anything regarding this potential issue.

As a part of the case introduction, the heat transfer assumptions were stated. When estimating production rates, the up-time of the system have been assumed to be 8760 hours during a year which is 100 %. This implies that no issues regarding liquid returns or that other problems related to the heat transfer mechanics occur. The difference between reality and theory would probably tell us that an assumption of 100 % up-time is way too optimistic. The same goes for heat pipe efficiency which also is assumed to be 1. This is however difficult to prove wrong without a proper test system where these things could be measured.

The heat exchanger that is supposed to take up heat extracted from the ground has a thermal efficiency of 50 %. This is a conservative value which most likely is possible to achieve higher with proper insulation, but chosen low deliberately as a safety factor to prevent unrealistically high production values. That specific assumption together with the assumption stating that

top side delivery infrastructure already was installed had to be made to narrow down the scope of this thesis.

The third and last thing to mention is that the heat exchanger possesses cooling water that has a temperature equal to the local ambient air temperature. This was done to get some constraints into the system, but this also means that during the summer season the air can reach temperatures above the temperature in the ground. When this happens, the heat transfer model predicts that the system will extract no heat at all, but rather cool down the water inside the heat exchanger. This alone adds great uncertainty to the production numbers and underlines the importance for good insulation around the heat exchanger and delivery infrastructure.

When considering the production numbers presented in the result section, the numbers are relatively high compared to what one could expect from a geothermal system installed in some of the coldest areas of the world. The heat production can supply 4 Norwegian homes with enough heat to cover all usage of electric energy to heating purposes. With very few analog systems to compare with it is difficult to say something about how realistic these are. In the eastern part of Norway, a geothermal heat pump was installed in 2016 where the drilled depth is the same as in the base case [20]. This heat pump system is installed to heat a nearby football field and the average estimated production for each well (two in total) was 120 000 to 150 000 kWh a year. Comparing this to 86 250 kWh from the base case makes the production numbers not that farfetched and can be considered reachable if a proper system is designed and presented issues avoided.

The production numbers make way for the profitability. As shown in plot 4 in the result section, the main cost driver is the drilling cost. The value of this cost was chosen in accord with what was presented in the article about the geothermal heat pump from eastern Norway. What the star diagram does not show is the sensibility toward material costs if a designer is forced to use a wick structure to ensure a more wetted pipe wall. This would drastically increase the material costs, but also reduce the hydraulic diameter of the pipe which affects the boiling area of the working fluid. Though the base case showed profitability, the pipe used was a simple steel pipe without any special features such as smoothened surface roughness. Based on this, the profitability of such a system would not only rely on reduced drilling costs,

but also costs related to materials that have been chosen in coordination with reliable test data from a similar test system. It is most likely to be more expensive than what the base case have shown.

The project cash flow is exclusively dependent on the electricity prices. In the results, the project net present value was compared against changes in the electricity pricing. Though the base case could handle a 30 % decrease in cash flow value, that analysis does not represent a thorough prediction of what the electricity prices would be during the project's life time which then again adds more uncertainty into what profitability can be expected. However, the economical evaluation of the systems profitability is considered accurate enough to point in the right direction whether this is something that should be built and tested to see if predicted production numbers are within reach.

It is worth mentioning that Enova provides economical support to systems that reduces greenhouse gas emissions and new technology [23]. As much as 60 % of the investment costs can be covered in loan by Enova to a discount rate of 1,29 % [24], which allows another potential investor risk less. There exists also other governmental subsidizing to systems that exploit renewable energy sources, but as to this date no subsidizing exists for a system described in this thesis.

8 Conclusion

When trying to give an answer to whether this type of geothermal system is a viable option to existing technology or not, the answer lies in the investigation performed during the base case and the economic analysis that followed. The heat transfer models that are available does not consider various production scenarios which may compromise the overall system output of heat. This adds a lot of uncertainties to how accurate the production numbers are. Because the case economics is based on how much heat that is possible to extract with the system, the economical aspect of this thesis also should be considered inaccurate to some extent.

The challenges when trying to implement heat pipes in geothermal wells will be to better understand the heat transfer through long adiabatic sections as well as materials selection for best possible return flow of condensed liquids. This means that such projects in best cases are marginal economically, and will rely on governmental support and funding.

The results found are still interesting enough to support the building of a deeper test system to develop better models and better overall understanding of the process. Ground source heat pipes seem to be a viable option to conventional heating systems, but also supplying relief to power grids delivering electric power. This is enough to look closer at these types of systems and it is strongly encouraged by the author of this thesis to do so.

List of references

[1] Lund, J. W. (2000). Taking the waters introduction to balneology. *Geo-Heat Center Bulletin*.

[2] Midtømme, K., & Nordgulen, Ø. (2000). *Markedsundersøkelse om geotermisk energi – geologiske forhold. Norwegian geological survey.*

[3] Barbier, E. (2002). Geothermal energy technology and current status: an overview. *Renewable and Sustainable Energy Reviews*, *6*(1), 3-65.

[4] Valdimarsson, P. (2011). Geothermal power plant cycles and main components. *Short Course on Geothermal Drilling, Resource Development and Power Plants", organized by UNU-GTP and LaGeo, in Santa Tecla, El Salvador*.

[5] Ramstad, R. K. (2011). Grunnvarme i Norge-Kartlegging av økonomisk potensial. *Report on commission*, *5*(2011), 87.

[6] Midttømme, K. (2005). Norway's geothermal energy situation. In *Proceedings*.

[7] Midtømme, K. (s.a.). *Geothermal energy in Norway*. Christian Michelsen Research Center.

[8] Korn, F. (2008). Heat pipes and its applications. *Heat and Mass Transport, Project Report*.

[9] Cengel, Y. A., & Boles, M. A. (2011). *Thermodynamics: An Engineering Approach Seventh Edition in SI Units.*

[10] Vasiliev, L. L. (2005). Heat pipes in modern heat exchangers. *Applied thermal engineering*, *25*(1), 1-19.

[11] Faghri, A. (2014). Heat pipes: review, opportunities and challenges. *Frontiers in Heat Pipes (FHP)*, *5*(1).

[12] Nguyen-Chi, H., & Groll, M. (1981). Entrainment or flooding limit in a closed two-phase thermosyphon. *Journal of Heat Recovery Systems*, *1*(4), 275-286.

[13] Shukla, K. N. (2015). Heat Pipe for Aerospace Applications—An Overview. *Journal of Electronics Cooling and Thermal Control*, *5*(01), 1.

[14] Lee, R. C., Nydahl, J. E., & Pell, K. M. (1986). *Design and implementation of a water powered pipe system for bridge heating. Final report.* (No. FHWA-WY-86-002).

[15] Zuo, Z. J., & Faghri, A. (1998). A network thermodynamic analysis of the heat pipe. *International Journal of Heat and Mass Transfer*, *41*(11), 1473-1484.

[16] Nydahl, J. E., Pell, K., & Lee, R. (1987). Bridge deck heating with ground-coupled heat pipes: analysis and design. *ASHRAE transactions*, *93*, 939-958.

[17] Lorentzen, P., Lysen, C., & Schreiner, J. (2013). *Mulighetsanalyse av vannkraftproduksjon i Smådalselva*. Bacheloroppgave ved Høgskolen i Bergen, Bergen.

[18] Elektrisitetspriser. SSB. Downloaded 5. May 2017 from: https://www.ssb.no/elkraftpris/

[19] Priseksempel på brønnboring. (s.a.). Downloaded 13. April 2017 from: http://www.xn--vrs-vlad.no/priseksempel_vann.html

[20] Lie, Ø. (2016, 14. april). Her borer de Norges dypeste energibrønn. Downloaded 26. April 2017 fra: https://www.tu.no/artikler/her-borer-de-norges-dypeste-energibronn/346350

[21] Price catalogue Norsk Stål. (2017). Downloaded 16. May 2017 from: http://pub.webbook.no/norskstaal/prisliste/#52/z

[22] Local average temperatures. Norwegian Meteorological Institute. Downloaded 20. May 2017 from: https://www.yr.no/sted/Norge/Hordaland/Bergen/Bergen_(Florida)_m%C3%A5lestasjon/statistikk.html

[23] Enova. (2017). Demonstrasjon av ny energi- og klimateknologi. Downloaded 1. June 2017 from: https://www.enova.no/bedrift/energisystem/ny-teknologi-i-energisystem/demonstrasjon-av-ny-energi---og-klimateknologi/

[24] Rates applicable to EFTA States under the state aid rules. (2017). Downloaded 1. June 2017 From: http://www.eftasurv.int/state-aid/rates/

Figure 1: Two phase heat transfer principles. (s.a). Downloaded 27. March 2017 from: https://home.ctw.utwente.nl/witsww/index.php/research/two-phase-principles

Figure 2: Bai, L., Lin, G., & Peterson, G. P. (2013). Evaporative heat transfer analysis of a heat pipe with hybrid axial groove. *Journal of Heat Transfer*, *135*(3), 031503.

Figure 3, 4 and 5:

Zuo, Z. J., & Faghri, A. (1998). A network thermodynamic analysis of the heat pipe. *International Journal of Heat and Mass Transfer*, *41*(11), 1473-1484.

Figure 6:

Lee, R. C., Nydahl, J. E., & Pell, K. M. (1986). *Design and implementation of a water powered pipe system for bridge heating. Final report.* (No. FHWA-WY-86-002).

Appendix A: Production numbers versus depth

TVD	Tground	ΔT	P (W)	E (t) (kWh)	E (10^3 kWh)
0	7,45	0,00	0,00	0,00	0,00
25,00	7,95	0,50	615,38	5390,76	2,70
50,00	8,45	1,00	1230,77	10781,51	5,39
75,00	8,95	1,50	1846,15	16172,27	8,09
100,00	9,45	2,00	2461,53	21563,03	10,78
125,00	9,95	2,50	3076,92	26953,79	13,48
150,00	10,45	3,00	3692,30	32344,54	16,17
175,00	10,95	3,50	4307,68	37735,30	18,87
200,00	11,45	4,00	4923,07	43126,06	21,56
225,00	11,95	4,50	5538,45	48516,82	24,26
250,00	12,45	5,00	6153,83	53907,57	26,95
275,00	12,95	5,50	6769,22	59298,33	29,65
300,00	13,45	6,00	7384,60	64689,09	32,34
325,00	13,95	6,50	7999,98	70079,85	35,04
350,00	14,45	7,00	8615,37	75470,60	37,74
375,00	14,95	7,50	9230,75	80861,36	40,43
400,00	15,45	8,00	9846,13	86252,12	43,13
425,00	15,95	8,50	10461,52	91642,88	45,82
450,00	16,45	9,00	11076,90	97033,63	48,52
475,00	16,95	9,50	11692,28	102424,39	51,21
500,00	17,45	10,00	12307,67	107815,15	53,91
525,00	17,95	10,50	12923,05	113205,91	56,60
550,00	18,45	11,00	13538,43	118596,66	59,30
575,00	18,95	11,50	14153,82	123987,42	61,99
600,00	19,45	12,00	14769,20	129378,18	64,69
625,00	19,95	12,50	15384,58	134768,93	67,38
650,00	20,45	13,00	15999,96	140159,69	70,08
675,00	20,95	13,50	16615,35	145550,45	72,78
700,00	21,45	14,00	17230,73	150941,21	75,47
725,00	21,95	14,50	17846,11	156331,96	78,17
750,00	22,45	15,00	18461,50	161722,72	80,86
775,00	22,95	15,50	19076,88	167113,48	83,56
800,00	23,45	16,00	19692,26	172504,24	86,25

Appendix B: System costs and net present value

TVD	E	Annual cash flow	Invesment	Net present value
0	0	kr 0	kr 14 000	kr -14 000,00
25,00	2695,3863	-kr 7 305	kr 47 043	kr -181 389,29
50,00	5390,7726	-kr 4 609	kr 80 085	kr -164 858,12
75,00	8086,1589	-kr 1 914	kr 113 128	kr -148 326,95
100,00	10781,5452	kr 782	kr 146 170	kr -131 795,79
125,00	13476,9315	kr 3 477	kr 179 213	kr -115 264,62
150,00	16172,3178	kr 6 172	kr 212 255	kr -98 733,45
175,00	18867,7041	kr 8 868	kr 245 298	kr -82 202,28
200,00	21563,0904	kr 11 563	kr 278 340	kr -65 671,12
225,00	24258,4767	kr 14 258	kr 311 383	kr -49 139,95
250,00	26953,863	kr 16 954	kr 344 425	kr -32 608,78
275,00	29649,2493	kr 19 649	kr 377 468	kr -16 077,61
300,00	32344,6356	kr 22 345	kr 410 510	kr 453,55
325,00	35040,0219	kr 25 040	kr 443 553	kr 16 984,72
350,00	37735,4082	kr 27 735	kr 476 595	kr 33 515,89
375,00	40430,7945	kr 30 431	kr 509 638	kr 50 047,05
400,00	43126,1808	kr 33 126	kr 542 680	kr 66 578,22
425,00	45821,5671	kr 35 822	kr 575 723	kr 83 109,39
450,00	48516,9534	kr 38 517	kr 608 765	kr 99 640,56
475,00	51212,3397	kr 41 212	kr 641 808	kr 116 171,72
500,00	53907,726	kr 43 908	kr 674 850	kr 132 702,89
525,00	56603,1123	kr 46 603	kr 707 893	kr 149 234,06
550,00	59298,4986	kr 49 298	kr 740 935	kr 165 765,22
575,00	61993,8849	kr 51 994	kr 773 978	kr 182 296,39
600,00	64689,2712	kr 54 689	kr 807 020	kr 198 827,56
625,00	67384,6575	kr 57 385	kr 840 063	kr 215 358,73
650,00	70080,0438	kr 60 080	kr 873 105	kr 231 889,89
675,00	72775,4301	kr 62 775	kr 906 148	kr 248 421,06
700,00	75470,8164	kr 65 471	kr 939 190	kr 264 952,23
725,00	78166,2027	kr 68 166	kr 972 233	kr 281 483,40
750,00	80861,589	kr 70 862	kr 1 005 275	kr 298 014,56
775,00	83556,9753	kr 73 557	kr 1 038 318	kr 314 545,73
800,00	86252,3616	kr 76 252	kr 1 071 360	kr 331 076,90

Appendix C: Bridge deck layout

System layout from Spring Creek, Wyoming [14].

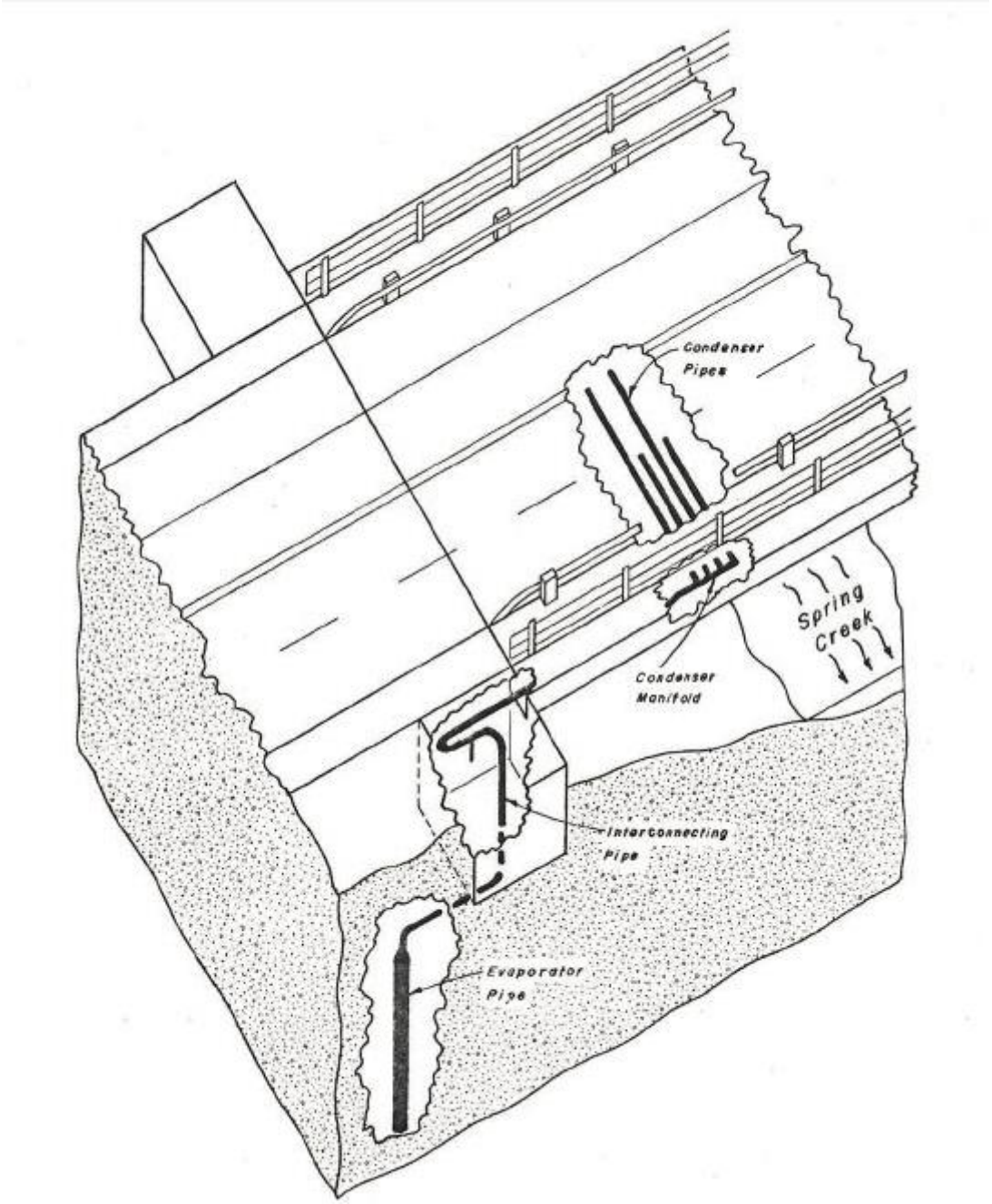

Appendix D

Electricity prices in the end-user market, quarterly. Øre/kWh

	4. quarter 2016	Change in percent	
	Øre/kWh	Last 3 md.	Last 12 md.
Households. Total price of electricity, grid rent and taxes	100,4	10,9	23,8
Electricity price	37,6	23,3	45,2
Grid rent	27,9	2,2	7,3
Taxes	34,9	6,7	19,5
Households. Electricity price by type of contract. Exclusive taxes			
New fixed-price contracts-1 year or less[1]	31,1	5,1	0
New fixed-price contracts-1 year or more[1]	29,9	-1,3	-3,9
All other fixed-price contracts	29,7	-0,3	-7,8
Contracts tied to spot price	36,6	25,8	51,2
Variable price (not tied to spot price)	40,6	18,4	37,6
Business activity. Electricity price. Exclusive taxes			
Services	35,5	30,5	42
Manufacturing excl. energy-intensive manufacturing	35	31,6	47,1
ManufacturiEnergy-intensive manufacturing	30	-0,3	-5,7

[1]New fixed-price contracts are entered into the last 3 months before the measuring period, and older fixed-price contracts are entered earlier.

Electricity prices including fees and taxes [18]

Appendix E

	Temperature			
	Average	Normal	Hottest	Coldest
Month				
apr.17	6,2	5,9	13,4° 30. apr	-0,9° 14. apr
mar.17	4,7	3,3	13,0° 28. mar	-3,3° 7. mar
feb.17	3	1,5	12,1° 3. feb	-6,7° 9. feb
jan.17	3,6	1,3	9,4° 29. jan	-6,5° 16. jan
des.16	6,1	2,4	11,3° 8. des	-1,3° 14. des
nov.16	4	4,6	11,6° 15. nov	-6,4° 8. nov
okt.16	8,3	8,6	17,7° 7. okt	1,3° 22. okt
sep.16	15,2	11,2	27,6° 16. sep	7,9° 4. sep
aug.16	14,2	14,1	24,5° 21. aug	6,7° 11. aug
jul.16	14,7	14,3	27,8° 21. jul	9,3° 7. jul
jun.16	15,3	13,3	27,8° 3. jun	6,9° 10. jun
mai.16	12,2	10,5	25,1° 9. mai	4,1° 14. mai
apr.16	6,2	5,9	14,9° 12. apr	-0,7° 24. apr

Temperatures from MET [22].

Appendix F: System schematics